AD-A136 223 A COMPARISON OF OPTICAL VERSUS HARDWARE FOURIER TRANSFORMS(U) VIRGINIA POLYTECHNIC INST AND STATE UNIV BLACKSBURG DEPT OF PHYSICS S P ALMEIDA 31 OCT 83 1/1

UNCLASSIFIED AFOSR-TR-83-1077 AFOSR-83-0200 F/G 12/1 NL

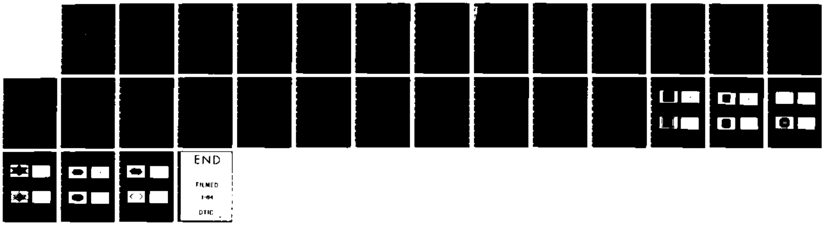

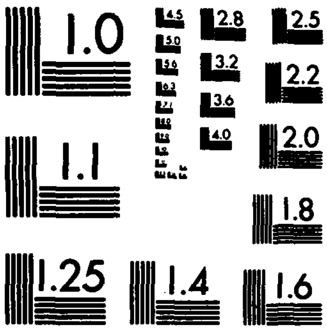

MICROCOPY RESOLUTION TEST CHART
NATIONAL BUREAU OF STANDARDS-1963-A

AFOSR-TR- 83-1077

AD-A136 233

Virginia Polytechnic Institute
and State University
Physics Department
Blacksburg, Virginia 24061

12

Submitted to
AIR FORCE OFFICE OF SCIENTIFIC RESEARCH
Final Technical Report
(Grant No. AFOSR-83-0200)
October 31, 1983

A COMPARISON OF OPTICAL VERSUS HARDWARE
FOURIER TRANSFORMS

by

Silverio P. Almeida

UNCLASSIFIED

SECURITY CLASSIFICATION OF THIS PAGE (When Data Entered)

REPORT DOCUMENTATION PAGE		READ INSTRUCTIONS BEFORE COMPLETING FORM
1. REPORT NUMBER AFOSR-TR- 83-1077	2. GOVT ACCESSION NO. AD A136 723	3. RECIPIENT'S CATALOG NUMBER
4. TITLE (and Subtitle) A comparison of optical versus hardware Fourier transforms		5. TYPE OF REPORT & PERIOD COVERED Final report 1 July 1983-31 Oct. 1983
		6. PERFORMING ORG. REPORT NUMBER
7. AUTHOR(s) Dr. Silverio P. Almeida		8. CONTRACT OR GRANT NUMBER(s) AFOSR-83-0200
9. PERFORMING ORGANIZATION NAME AND ADDRESS Virginia Polytechnic Institute and State University Contract and Grant Administration, 301 Burruss Hall Blacksburg, VA 24061		10. PROGRAM ELEMENT, PROJECT, TASK AREA & WORK UNIT NUMBERS 61102F 2305/D9
11. CONTROLLING OFFICE NAME AND ADDRESS AFOSR/[redacted] NE Building 410 Bolling AFB, DC 20322		12. REPORT DATE October 31, 1983
		13. NUMBER OF PAGES 28
14. MONITORING AGENCY NAME & ADDRESS (if different from Controlling Office) AFOR/NE Building 410 Bolling AFB, DC 20332		15. SECURITY CLASS. (of this report) Unclassified
		15a. DECLASSIFICATION DOWNGRADING SCHEDULE

16. DISTRIBUTION STATEMENT (of this Report)

Approved for public release; distribution unlimited.

17. DISTRIBUTION STATEMENT (of the abstract entered in Block 20, if different from Report)

18. SUPPLEMENTARY NOTES

AFOSR Final Report

19. KEY WORDS (Continue on reverse side if necessary and identify by block number)

Optical Fourier Transforms
Array Processing of Fast Fourier Transform
Spatial Filtering

20. ABSTRACT (Continue on reverse side if necessary and identify by block number)

A comparison of the optical transform versus the hardware Fourier transform was made for two input functions: a rectangular aperture and a six-pointed star design. The optical transforms were modified using sharp and smooth low-pass as well as highpass filters. The results were compared against those obtained using the array processor hardware at the Brooks Air Force Base, School of Aerospace Medicine. The "ringing" observed in the lowpass filtered results of the array processor was simulated by the optical methods. However, certain asymmetries in the hardware "ringing" data were not observed optically.

ABSTRACT

A comparison of the optical transform versus the hardware Fourier transform was made for two input functions: a rectangular aperture and a six-pointed star design. The optical transforms were modified using sharp and smooth lowpass as well as highpass filters. The results were compared against those obtained using the array processor hardware at the Brooks Air Force Base, School of Aerospace Medicine. The "ringing" observed in the lowpass filtered results of the array processor was simulated by the optical methods. However, certain asymmetries in the hardware "ringing" data were not observed optically. A discussion of the "ringing" and how to eliminate it is also presented.

TABLE OF CONTENTS

LIST OF FIGURES

I. INTRODUCTION

The main purpose of this research is to compare the Fourier transform and its inverse filtered Fourier transform obtained with the Digital Image Processing (DIP) hardware system located at the School of Aerospace Medicine, Brooks Air Force Base, San Antonio, Texas against the optical version of the transforms obtained at the Virginia Tech coherent optics laboratory. The Air Force test patterns consisted of a rectangular aperture and a six-pointed star design. They were both recorded on 35 mm transparencies, and provided to us by Dr. Ralph G. Allen, Director of the Laser Effects Branch (Division of Radiation Sciences). The DIP system consisted of: an Analogic array processor on-line to an Aydin monitor and a PDP-11-32 mini-computer system. Both the rectangular aperture and six-pointed star design were digitized (512x512) pixels and entered into the Analogic array processor which performed the hardware Fourier transform (HFT). This HFT was then operated on with lowpass and highpass Modulation Transfer Functions (MTF); next the inverse hardware Fourier transform (IHFT) was performed. The Aydin monitor was used to display the HFT and the IHFT. The results were photographs of the Aydin monitor screen displays and recorded on 35 mm transparencies. It is this set of transparencies including: the original input designs (rectanuglar aperture and six-pointed star); the HFT and IHFT that we wished to compare against their optical equivalents. In some cases we were able to duplicate the hardware results using optical methods. In those instances where differences in the two methods were observed we have recorded the differences with explanations for them.

It is important to test the DIP system Fourier transform capabilities against the optical (traditional) methods. The DIP system could be very useful for on-line filtering (Modulation Transfer Manipulation) of images and rapid analysis.

II. OPTICAL FOURIER TRANSFORMS: OFT

A two dimensional Fourier transorm can be performed using a convergent lens and coherent illumination of the input pattern[1]. Various optical set-ups can be implemented to carry our the OFT. For this experiment we have chosen a converging beam[2] approach rather than the classical 2-f configuration[3]. Both methods are equivalent for our purposes as is shown in ref. (2). Figures (1, 2) show the converging beam schematic used to obtain the OFT. The high and lowpass spatial frequency filters were located on glass microscope slides as either a black dot (highpass) or a black annulus (lowpass) and positioned in the Fourier transform plane via micrometers with X-Y movements. Since the exact MTF cut-off frequencies used in the IHFT are unknown for the transparencies provided to us, we have tried various optical pass filters in order to simulate these results.

A. Rectangular aperture Fourier transform theory

The analytic treatment of the OFT can be outlined as follows[1,2]. Given a rectangular aperture whose amplitude transmittance is given by

$$t(x_o,y_o) = \mathrm{rect}\left(\frac{x_o}{L_x}\right) \mathrm{rect}\left(\frac{y_o}{L_y}\right) \tag{1}$$

where

$$\mathrm{rect}\,(x_o) = \begin{cases} 1 & |x_o| \leq \frac{1}{2} \\ 0 & \text{elsewhere} \end{cases} \qquad \mathrm{rect}(x_o) = \begin{cases} 1 & |x_o| \leq \frac{1}{2} \\ 0 & \text{elsewhere} \end{cases}$$

and similarly for rect (y_o). L_x, L_y represent the aperture widths in the x_o and y_o directions, respectively. Assume that the pupil function $P(x_o, y_o) = 1$ since $x_o^2 + y_o^2 < a^2$ where a = radius of the lens; also that the amplitude illumination is unity (i. e. A=1). Then in the Fresnel approximation the field distribution in the Fourier transform plane $g_2(x_f, y_f)$ is given by:

$$g_2\,(x_f, y_f) = \frac{A \exp\,[i\,\frac{k}{2d}(x_f^2 + f_y^2)]}{i\lambda d}\,(\frac{f}{d})\,.$$

$$\iint_{-\infty}^{\infty} t(x_o, y_o)\,P(x_o, y_o)\exp\,[-i\frac{k}{d}\,(x_o x_f + y_o y_f)]\,dx_o dy_o \tag{2}$$

$$= \frac{\exp\,[i\,\frac{k}{2f}\,(x_f^2 + y_f^2)]}{i\lambda f}\,F[t(x_o, y_o)]$$

where $A \equiv 1$ (amplitude transmittance),

$P \equiv 1$ (pupil function)

$f = d$ (input plane is assumed to be next to the backside of the lens; $f \approx d$). f is the focal length of the lens.

The Fourier transform of the transmittance function $t(x_o,y_o)$ is given by

$$F[t(x_o, y_o)] = L_x L_y \operatorname{sinc}(L_x f_x) \operatorname{sinc}(L_y f_y) \tag{3}$$

where: $f_x \equiv (\frac{x_f}{\lambda f})$; $f_y \equiv (\frac{y_f}{\lambda f})$

are the spatial frequencies, some of which will be passed via the previously mentioned low and highpass filters. We now get that the Fourier transform of the rectangular aperture is given by

$$g_2(x_f, y_f) = \frac{\exp[i \frac{k}{2f}(x_f^2 + y_f^2)]}{i\lambda f} L_x L_y \operatorname{sinc}(L_x f_x) \operatorname{sinc}(L_y f_y) \tag{4}$$

The photograph representing this Fourier transform is, however, a square-law detector. That is, it records the intensity distribution of (4) given by:

$$I_{Rect}(x_f, y_f) = \frac{L_x^2 L_y^2}{\lambda^2 f^2} \operatorname{sinc}^2 (\frac{L_x x_f}{\lambda f}) \operatorname{sinc}^2 (\frac{L_y y_f}{\lambda f}) \tag{5}$$

B. Star Aperture Fourier transform theory

The six-pointed star can be treated as a two dimensional triangle function. That is, by using the following Fourier transform properties:

(a) Rotation: $f(r, \theta + \theta_0) \leftrightarrow F(\omega, \phi + \theta_0)$

(b) Distributive: $F\{f_1(x,y) + f_2(x,y)\} = F\{f_1(x,y)\} + F\{f_2(x,y)\}$

(c) Scaling: $f(ax, by) \leftrightarrow \frac{1}{|ab|} F \left(\frac{f_x}{a}, \frac{f_y}{b}\right)$

(d) Translation: $f(x-x_o, y-y_o) \leftrightarrow F(f_x, f_y) \exp\left[-i2\pi(f_x x_o + f_y y_o)\right]$.

The triangle function tri(x), tri(y) is defined as:

$$\mathrm{tri}\,(x) = \begin{cases} 1 - |x| & |x| \leqslant 1 \\ 0 & \text{elsewhere} \end{cases}$$

$$\mathrm{tri}\,(y) = \begin{cases} 1 - |y| & |y| \leqslant 1 \\ 0 & \text{elsewhere} \end{cases}$$

Equation (2) for the Fourier transform and its associated conditions for the pupil function, unit amplitude and f=d can be applied to the two-dimensional triangle function where now we let $t(x_o,y_o)$ be the amplitude transmittance.

$$t(x_o,y_o) = \mathrm{tri}\,(x_o)\ \mathrm{tri}\,(y_o) \tag{6}$$

then the Fourier transform becomes

$$g_2(x_f,y_f) = \frac{A \exp\left[i \frac{k}{2f}(x_f^2 + y_f^2)\right]}{i\lambda f} F\left\{t(x_o,y_o)\right\} \tag{7}$$

where:

$$F\left\{t(x_o,y_o)\right\} = \mathrm{sinc}^2\,(f_x)\ \mathrm{sinc}^2\,(f_y) \tag{8}$$

and again: $f_x \equiv (\frac{x_f}{\lambda f})$; $f_y \equiv (\frac{y_f}{\lambda f})$

are the spatial frequencies. f = focal length of the converging lens; λ = wavelength of Helium-Neon laser; x_f and y_f are coordinate positions in the Fourier transform plane. Since we measure (photograph) the intensity distribution of $g_2(x_f,y_f)$ we can neglect the quadratic phase factor that appears in eq (2) and (7). The resulting intensity for the triangle function becomes

$$I_{Tri}(x_f,y_f) \simeq \{\text{Sinc}^2\ (f_x)\ \text{Sinc}^2\ (f_y)\}^2 \tag{9}$$

C. Lowpass filter "ringing"

It is noticed that considerable amount of "ringing" and some blurring of inverse Fourier transform images occurs when sharp lowpass frequency cut-off filters are used. This effect is seen in the results of the Analogic array processor IHFT images. We too were able to simulate this "ringing" with our sharp lowpass optical filters. A sharp lowpass filter (SLPF) can be represented by a transfer function $H(u,\nu)$ in the Fourier transform plane, where

$$H(u,\nu) = \begin{cases} 1 & r(u,\nu) < r_o \\ 0 & r(u,\nu) > r_o \end{cases} \tag{10}$$

r_o is the radius of the rectangle function. The complete function is obtained by rotating the rect function about its axis. This generates an "ideal" lowpass filter with sharp edges. The radius of the filter is given by

$$r_o = [u^2 + \nu^2]^{1/2} \tag{11}$$

This circle super-imposed on the Fourier transform plane (concentric with it) provides the interior zone for passing the low frequencies. As r_o is increased higher frequencies are passed; eventually r_o is so large that all frequencies pass.

The "ringing" phenomenon can be discussed in terms of the convolution theorem. In the frequency plane we have that

$$G(u,\nu) = H(u,\nu)\ F\ (u,\nu) \tag{12}$$

where:

$H(u,\nu)$ = transfer function and $F(u,\nu)$ = Fourier transform of the input function $f(x,y)$. Using the convolution theorem one gets

$$g(x,y) = h(x,y) * f(x,y) \tag{13}$$

where

$g(x,y)$ = output function and $h(x,y)$ = inverse Fourier transform of the transfer function. Since the transfer function is the rectangle function its inverse is the sinc function. Therefore, the convolution of this sinc function with $f(x,y)$ will yield a series of rings depending on the radius of $h(u,v)$. The number of rings produced is inversely proportional to the radius of $H(u,v)$. For lowpass filtering more ringing occurs as the radius gets smaller. When the radius of $H(u,v)$ is large enough to include all the high frequencies the ringing disappears; but so does the lowpass filtering effect.

D. Elimination of "ringing"

It is possible to lessen or remove the ringing in lowpass filtering. The method is basically one of smoothing the edges of the lowpass filter. Special filters can be constructed for this purpose. We shall give three examples of such filters.

(1) Butterworth lowpass filter (BLPF)

$$H(u,v) = \frac{1}{1 + [r(u,v)/r_o]^{2n}} \tag{14}$$

where the order of the transfer function $H(u,v)$ is given by n; r_o is the cut-off frequency. By rotating the $H(u,v)$ function about its axis one gets the three-dimensional form.

(2) Exponential lowpass filter (ELPF)

$$H(u,v) = \exp - [r(u,v)/r_o]^n \tag{15}$$

where n controls the rate of decay.

(3) Trapezoidal lowpass filter (TLPF)

$$H(u,v) = \begin{cases} 1 & r(u,v) < r_o \\ \frac{1}{(r_o - r_1)} [r(u,v) - r_1] & r_o \leq r(u,v) < r_1 \\ 0 & r(u,v) > r_1 \end{cases} \qquad (16)$$

The three examples given above (BLPF, ELPF and the TLPF) are, in effect, smoothing the edge of the lowpass filter by allowing a small portion of the higher frequencies to pass. This help to eliminate both the ringing and blurring.

III. EXPERIMENTAL RESULTS

Shown in figures (3 - 8) are the results of the comparison between the hardware Analogic array processor Fourier transforms and those obtained using optical Fourier transform methods. In order to better compare the two methods the 35 mm Air Force transparancies (negatives) were converted into positives as ours were before printing the hardcopy photographs. In this way the backgrounds for both cases is the same (i.e. dark).

Figure (3) shows the Air Force results obtained for the square aperture input using the Analogic array processor. Figure (3b) is the HFT (hardware Fourier transform) of the square aperture in (3a). This result is consistent with its optical counterpart OFT (optical Fourier transform) as shown in fig. (4b) for the square aperture input (4a). Only a slight scale size difference is observed due to the smaller square used in (4a). The slightly smaller square was used in the optical set-up in order to utilize the center of the lens and thereby eliminate possible aberrations. Figure (3c) shows the IHFT (inverse hardware Fourier transform) of the lowpass filtered Fourier transform shown in (3d). The optical comparison is shown respectively in figure (4c) and (4d). Some differences are observed in these two methods and are as follows: (1) more internal "ringing" is shown in IHFT (3c) than the IOFT (4a). This could be due to the fact that when photographing (4c) the optical IOFT the film quickly saturates in intensity at the center, thereby giving the "ringing" less contrast. However, in the IHFT the displayed results were presented in the logarithmic scale thereby enhancing the "ringing". Visually we observed the same "ringing" phenomenon. The asymmetry is the "ringing" shown in figure (3c) IHFT was, however, not observed. We believe this could be due either to a hardware or software problem. Another possibility is when the square aperture was digitized for input to the Analogic array processor it is possible the illumination of the 35 mm transparency was not uniform.

The IOFT (inverse optical Fourier transform) of the highpass filter shown in fig (5d) is presented in (5c). Again "ringing" and harmonic mode oscillations of the "ringing" are observed in the optical case. The hardware IHFT filter shown in fig (5a) is for the highpass filter in (5b). Although some edge "ringing" is observed we do not see the same interior mode "ringing" observed optically. We believe that either fig (5a) is not the actual IHFT of (5b) or the exposure of (5a) was not presented on a logarithmic scale as was done for fig (3c) in the lowpass IHFT.

The six-pointed star aperture and its hardware Fourier transform are shown in fig (6a) and (6b) respectively. The lowpass IHFT of the star is shown in fig (6c). Again one observed the "ringing" as well as some asymmetry in the "ringing" in the inner-most rings. The optical results to compare against the star are shown in fig (7). In this case a clear cut-out of a hexagon was used to simulate the star shwon in fig (6a). This hexagon fig (7a) via the Fourier theorems (discussed earlier) should replicate to a good approximation fig (6a). It was also easier to fabricate accurately than a six-pointed star. The optical Fourier transform of (6a) is shown in fig (6b). The inverse optical Fourier transform for the low-pass filter is given in fig (7a). "Ringing" is observed as before and due to intensity saturation the central "ringing" observed visually did not photograph well. Again, we did not observe any asymmetry in the central region as seen on the logarithmic scale in fig (6c). We believe, as before, that this asymmetry is the result of non-uniform illumination; hardware or software problems in the array processor system.

The high and lowpass optical filters used were proportionaly the same size as those used in the hardware analysis. We tried to use (roughly) the same frequency cut-offs in both cases. In addition we tried to eliminate observed "ringing" by using smooth high and lowpass optical filters instead of sharp ones. Figures (8a) and (8c) show the inverse Fourier transforms after using the smooth filters on (8b) and (8d) respectively. One observes that the "ringing" nearly disappears. These filters were produced by allowing a slight blurring of the boundary between the opaque and transparent regions on the glass filter slide. The results obtained are discussed further in the next section.

IV. DISCUSSION AND CONCLUSION

The comparison of the optical Fourier transform against the Analogic array processor Fourier transform of the square and star aperture showed that both similarities and some differences were present. We shall discuss each separately and draw some conclusions.

A. Simularities

The Fourier transforms of both the square and star were essentially the same for the HFT and OFT methods. There are advantages in the hardware method when displaying the logarithmic of the intensity rather than a photograph of the Fourier/or inverse/ transform. Both methods also displayed "ringing" in their inverse low and highpass filtered transforms. The relative size of the low and highpass filters was about the same for both methods.

B. Differences

The amount of "ringing" varied in both methods. Here the "ringing" could be better observed when displayed by the hardware (logarithmic) method. Variations in the amount of "ringing" really depend on the exact frequency cut-off for the low and highpass filters. The precise cut-offs could not be easily matched since we were not given any data on the hardware parameters. The important point is that for the sharp cut-off frequencies "ringing" was observed in both cases. However, an important difference is the observed asymmetry in the "ringing" in the hardware method. This asymmetry was not observed at all in the optical method.

Some conclusions can be drawn from this comparison. The "ringing" observed is to be expected based on the so-called Gibbs phenomenon. The error due to the Gibbs "ringing" depends on where one truncates the frequency spectrum before performing the inverse Fourier transform. The inclusion of more high order frequencies greatly reduces the "ringing". When performing both low and highpass filtering the "ringing" can be minimized by using a "smooth" filter as discussed earlier in this report. For example, an array processor could program into its filtering an exponential decay curve which would pick up small amounts of high frequencies. The asymmetry in the "ringing" should be further studied to determine its exact cause. This requires the array processor which we do not have in our laboratory. There are pros and cons for each method. For example, the optical Fourier transform due to its parallel processing is faster than the array processor, given an input transparency one can readily get its optical F. T. using a rather inexpensive lens. An array processor would be a considerably more expensive method to get a simple F. T. of an image. On the other hand, manipulation of the Fourier transform plane with various Modulation Transfer Functions (so long as they can be obtained analytically) is easier (and more accurate) to perform with the array processor. Finally, the DIP system is a potentially powerful and important digital image processing system capable of many detailed Fourier transform studies. It should, however, be further compared against optical methods as indicated by this preliminary research study.

References

1. D. Joyeux and S. Lowenthal, Applied Optics, Vol. 21, No. 23 pp 4368-4372 (1982).

2. Srisuda Puang-ngern and Silverio P. Almeida pre-print; submitted to American Journal of Physics, Sept. 1983.

3. J. W. Goodman, Introduction to Fourier Optics)McGraw-Hill, New York, N. Y. 1968).

4. H. Stark, Applications of Optical Fourier Transforms (Academic Press, New York, N.Y. 1982)

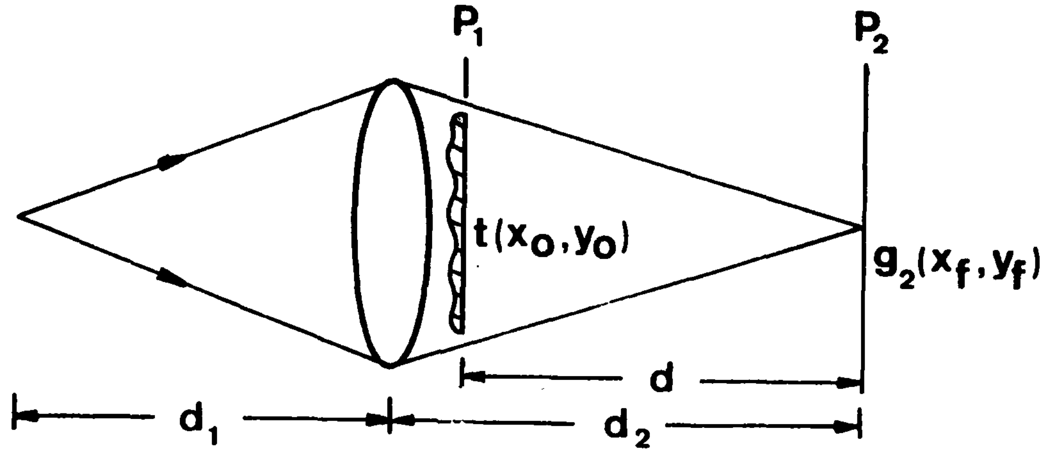

Converging beam optical Fourier transform set-up p_1 is input plane. p_2 the Fourier transform and filter plane.

Figure (1)

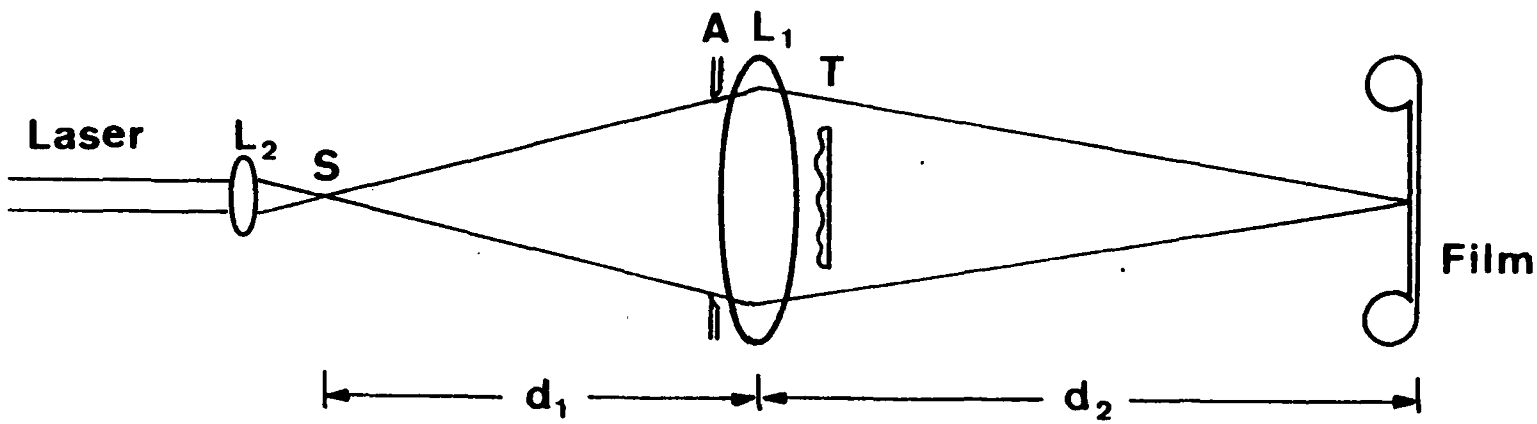

S is the coherent light point source. A is the aperture. L_1 is the Fourier transform lens. T the input object (square and star apertures). The Fourier transform is recorded on film at a distance d_2 from L_1.

Figure (2)

<u>Analogic Array Processor Results</u>
(Air Force Hardware)

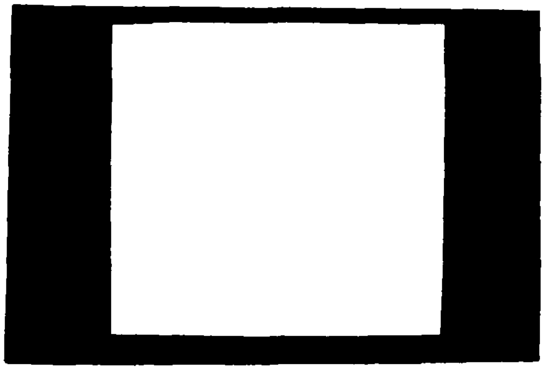

(a)
Square aperture input
(Air Force)

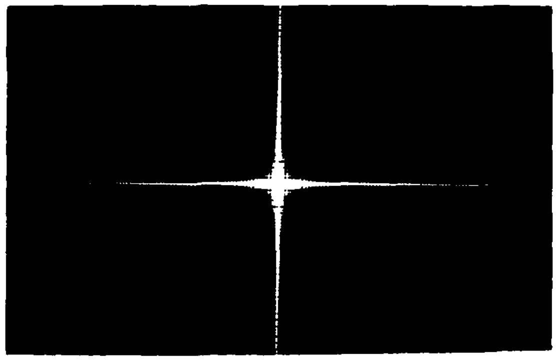

(b)
Fourier transform of
square aperture (a).

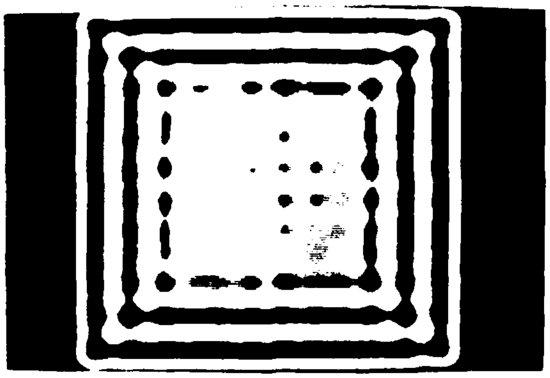

(c)
Inverse Fourier transform
of lowpass filtered FT
(b).

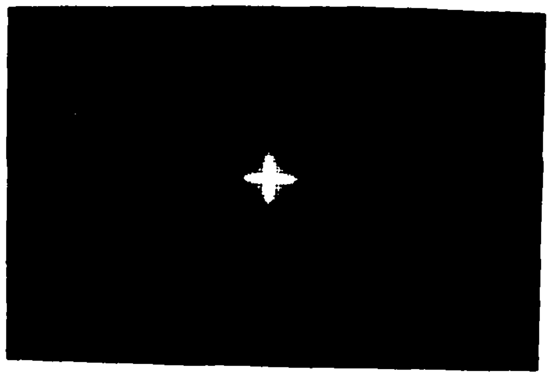

(d)
Lowpass filter used
on Fourier transform
(b).

Figure (3)

Optical Processor Results

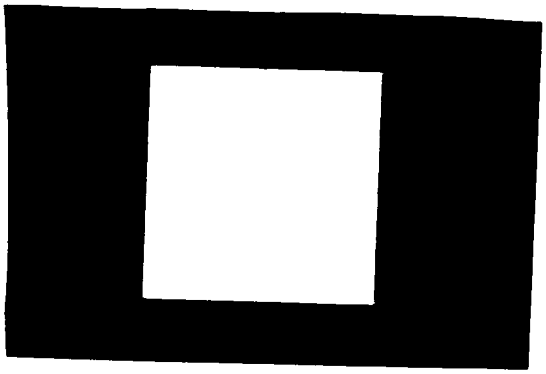

(a)

Square aperture input
(Virginia Tech.)

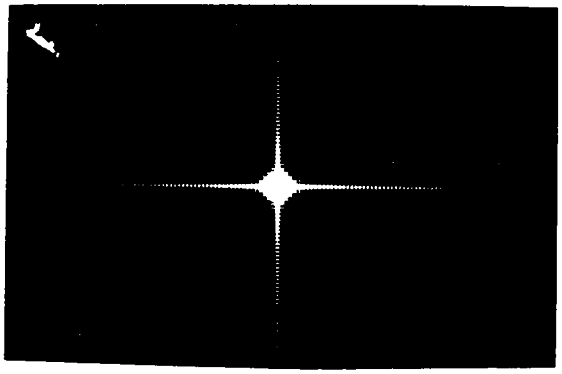

(b)

Fourier transform of
square aperture (a).

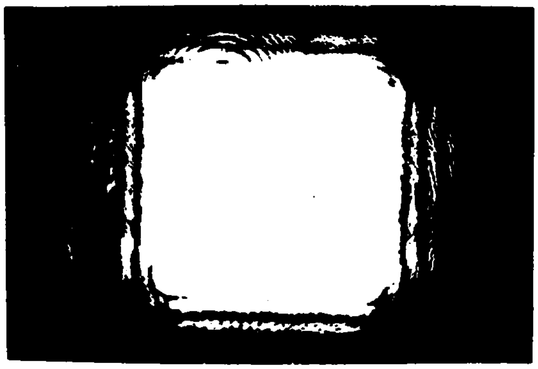

(c)

Inverse Fourier transform
of lowpass filtered FT (b).

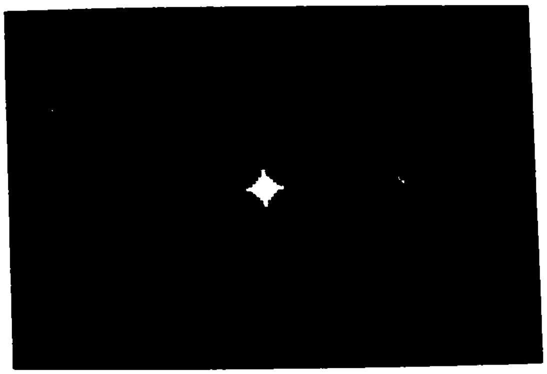

(d)

Lowpass filter used on
Fourier transform (b).

Figure (4)

Analogic Array Processor Results (a,b)
(Air Force Hardware)

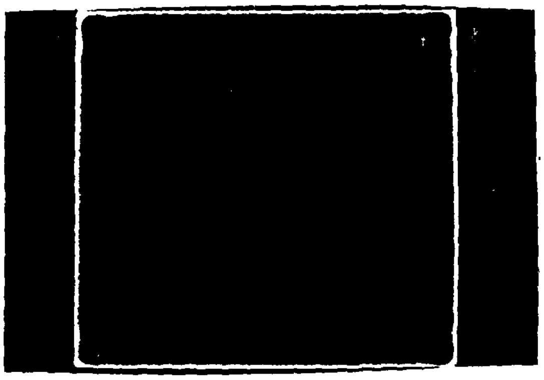

(a)
Inverse Fourier transform
of highpass filtered FT
Shown in Fig. (3b).

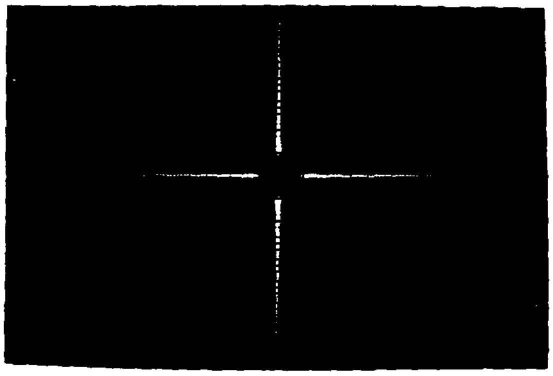

(b)
Highpass filter used
on Fourier transform
Fig. (3b)

Optical Processor Results (c,d)

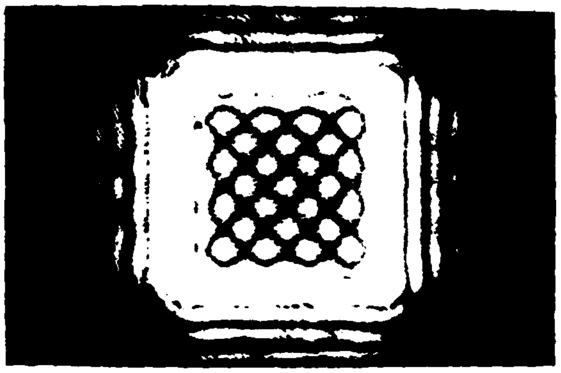

(c)
Inverse Fourier transform
of highpass filtered FT
shown in Fig. (4b).

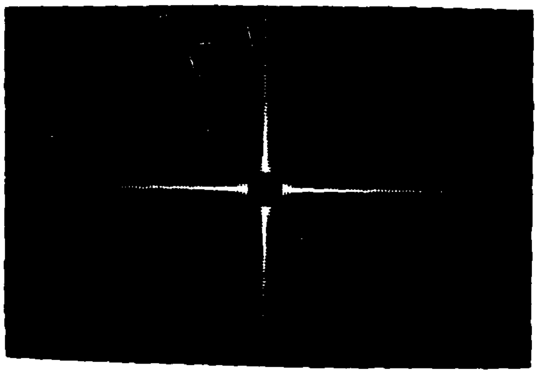

(d)
Highpass filter used
on Fourier transform
Fig. (4b).

Figure (5)

Analogic Array Processor Results
(Air Force Hardware)

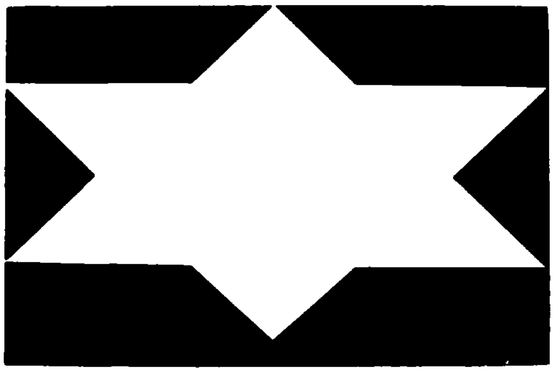

(a)
Star aperture input
(Air Force)

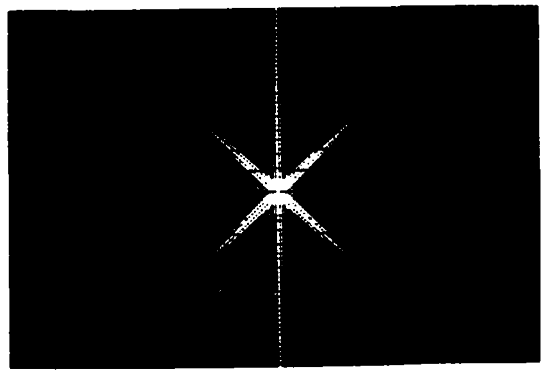

(b)
Fourier transform of
star aperture (a)

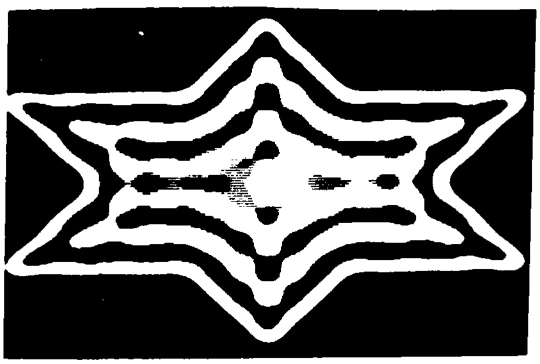

(c)
Inverse Fourier transform
of lowpass filtered FT (b).

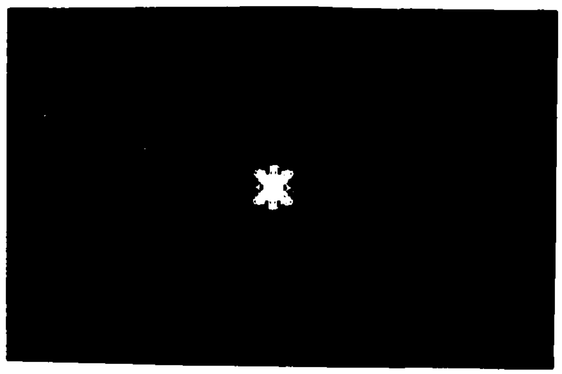

(d)
Lowpass filter used
on Fourier transform
(b).

Figure (6)

Optical Processor Results

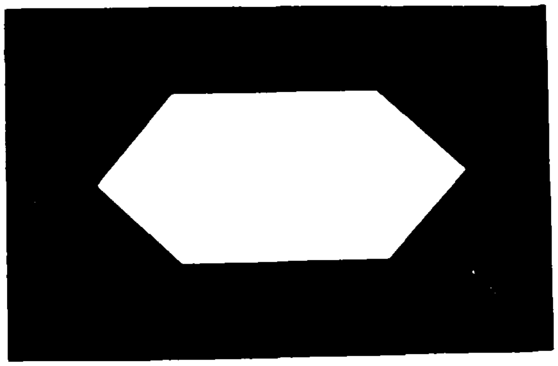

(a)

Simulated star aperture.

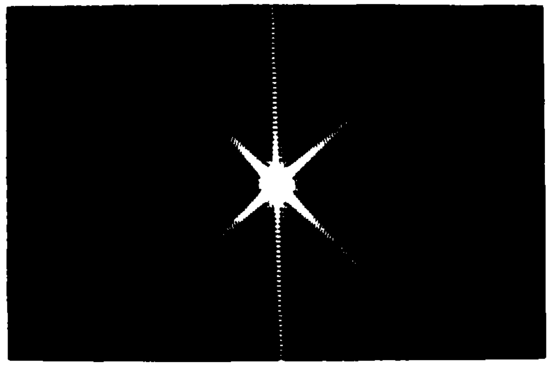

(b)

Fourier transform of simulated star aperture (a).

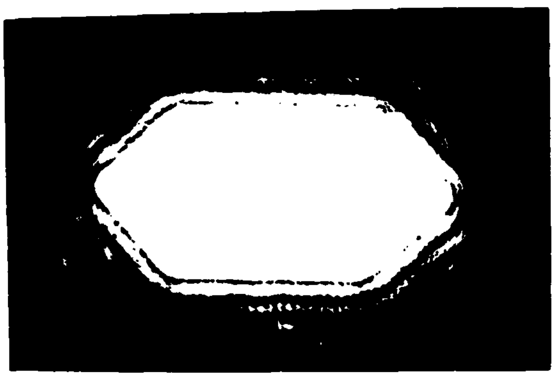

(c)

Inverse Fourier transform of lowpass filtered FT (b).

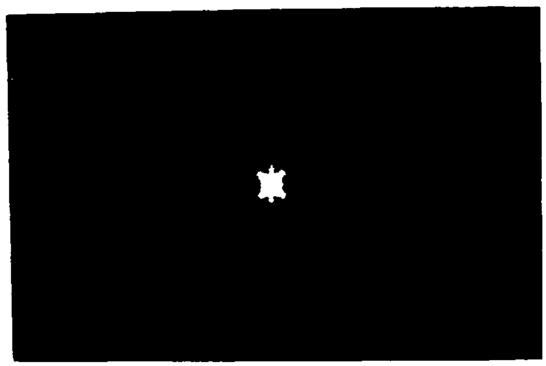

(d)

Lowpass filter used on Fourier transform (b).

Figure (7)

Optical Processor Results

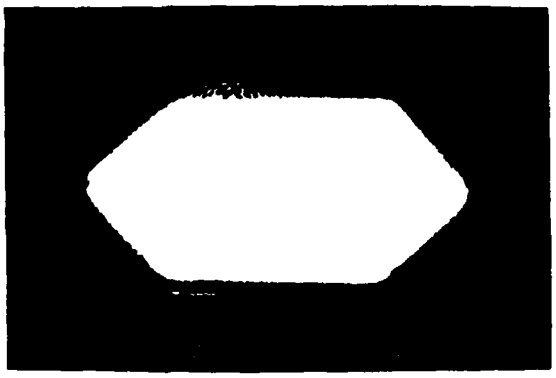

(a)
Inverse Fourier transform of smooth lowpass filtered FT shown in Fig. (7b).

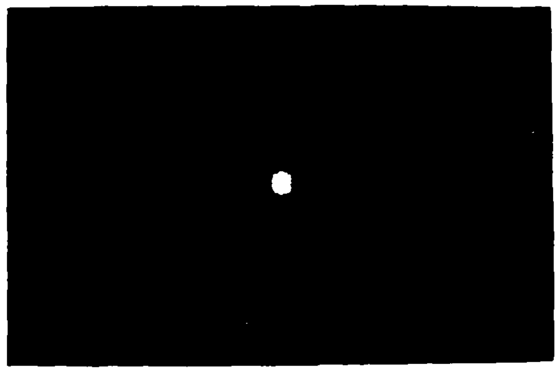

(b)
Smooth lowpass filter used on FT shown in Fig (7b) for simulated star aperture.

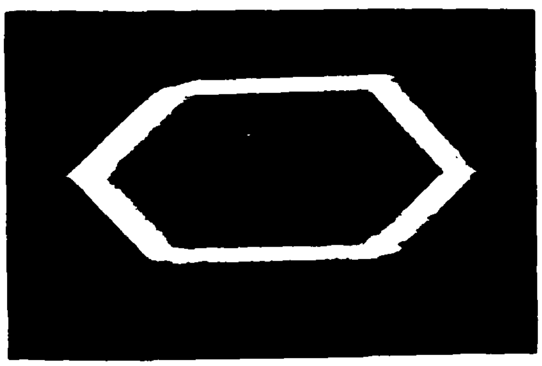

(c)
Inverse Fourier transform of smooth highpass filtered FT shown in Fig. (7b).

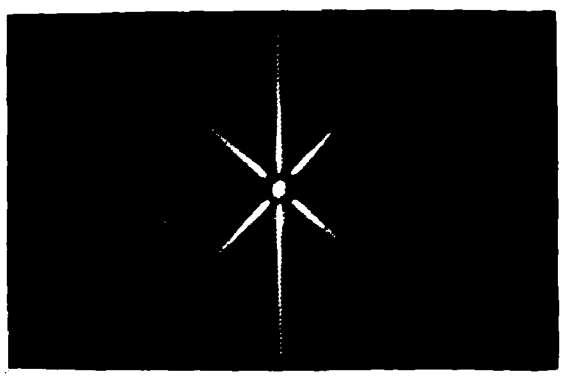

(d)
Smooth highpass filter used on FT shown in Fig (7b) for simulated star aperture.

Figure (8)

END

FILMED

1-84

DTIC